ФІЗИЧНІ, ХІМІЧНІ ТА ІНШІ ЯВИЩА, НА ОСНОВІ ЯКИХ МОЖУТЬ БУТИ СТВОРЕНІ СЕНСОРИ

PHYSICAL, CHEMICAL AND OTHER PHENOMENA, AS THE BASES OF SENSORS

MAGNETORESISTANCE AT ROOM TEMPERATURE IN THE A-SITE ORDERED $Pr_{0.70}Ba_{0.30}MnO_{3+\delta}$ MANGANITES

S. V. Trukhanov[1*], A. V. Trukhanov[1], C. E. Botez[2], H. Szymczak[3]

[1]Scientific-Practical Materials Research Centre NAS of Belarus, 220072 Minsk, P. Brovka str. 19, Belarus
(*e-mail : truhanov@ifttp.bas-net.by)
[2]University of Texas at El Paso El Paso, TX 79968-0515, USA
[3]Institute of Physics of PAS, 02-668 Warsaw, Poland

Abstract. The structure and magnetotransport properties of the *A*-site ionic ordered state in $Pr_{0.70}Ba_{0.30}MnO_{3+\delta}$ ($\delta = 0$, 0.025) have been investigated. The parent A-site ionic disordered $Pr_{0.70}Ba_{0.30}MnO_3$ compound is an orthorhombic (SG = Imma, Z = 4) ferromagnet with Curie temperature $T_C \approx 173$ K. It exhibits two peaks of electrical resistivity, at $T_I \sim 128$ K and $T_{II} \sim 173$ K, as well as two peaks of magnetoresistance ~ 74 % and ~ 79 % in a field of 50 kOe. The parent A-site ionic disordered $Pr_{0.70}Ba_{0.30}MnO_3$ sample used in our studies has an average grain size $\langle D \rangle \approx 10.213$ μm. Successive annealing of this sample in vacuum $P[O_2] \approx 10^{-4}$ Pa and then in air at T = 800 ⁰C leads to the destruction of its initial grain structure and to its chemical separation into two phases: (i) oxygen stoichiometric A-site ordered $PrBaMn_2O_6$ with tetragonal (SG = P4/mmm, Z = 2) unit cell and $T_C \approx 313$ K and (ii) oxygen superstoichiometric A-site disordered $Pr_{0.90}Ba_{0.10}MnO_{3.05}$ with orthorhombic (SG = Pnma, Z = 4) unit cell and $T_C \approx 133$ K. It also exhibits a magnetoresistance of ~ 14 % at ~ 313 K in a field of 50 kOe. This processed sample has a reduced average grain size $\langle D \rangle \approx 491$ nm. The observed magnetic properties are interpreted in terms of chemical phase separation, grain size, and A-site ionic ordering effects. The materials obtained in this work may be used at the creation of the magnetic field sensors, as they have considerable magnetoresistance (~14% in field of 50 kOe) at room temperature.

Keywords : cation ordering, manganites, magnetoresistance.

МАГНІТООПІР ПРИ КІМНАТНІЙ ТЕМПЕРАТУРІ В МАНГАНІТАХ $Pr_{0.70}Ba_{0.30}MnO_{3+\delta}$ З УПОРЯДКУВАННЯМ В А-ПОЗИЦІЇ

С. В. Труханов, А. В. Труханов, С. Е. Botez, H. Szymczak

Анотація. Досліджено структуру та магнітотранспортні властивості впорядкованого стану в А-позиції в манганітах $Pr_{0.70}Ba_{0.30}MnO_{3+\delta}$ ($\delta = 0, 0.025$). Вихідний розупорядкований в А-позиції склад $Pr_{0.70}Ba_{0.30}MnO_3$ є орторомбічним (SG = Imma, Z = 4) феромагнетиком з температурою Кюрі $T_C \approx 173$ K. Він проявляє два піки електричного опору при $T_I \sim 128$ K і $T_{II} \sim 173$ K, а також два піки магнітоопору ~ 74 % і ~ 79 % у полі 50 кЕ. Цей зразок $Pr_{0.70}Ba_{0.30}MnO_3$ складається з кристалітів із середнім розміром $\langle D \rangle \approx 10.213$ μm. Послідовний відпал цього зразка у вакуумі $P[O_2] \approx 10^{-4}$ Па, а потім на повітрі при $T = 800\ ^0C$ веде до руйнування його початкової структури і хімічному розшарування на дві фази: (i) стехіометричну по кисню впорядковану в А-позиції $PrBaMn_2O_6$ з тетрагональною (SG = P4/mmm, Z = 2) елементарною коміркою і $T_C \approx 313$ K і (ii) надстехіометричною по кисню розупорядкованою в А-позиції $Pr_{0.90}Ba_{0.10}MnO_{3.05}$ з орторомбічною (SG = Pnma, Z = 4) елементарною коміркою і $T_C \approx 133$ K. Він також проявляє магнітоопір ~ 14 % при ~ 313 K у полі 50 кЕ. Цей зразок складається із кристалітів зі зменшеним середнім розміром $\langle D \rangle \approx 491$ nm. Спостережувані магнітні властивості інтерпретуються в припущенні хімічного фазового розшарування, а також ефектів розмірності кристалітів і впорядкування катіонів в А-позиції. Отримані в даній роботі матеріали можуть бути використані при створенні датчиків магнітного поля, тому що володіють значним магнітоопором (~14% у полі 50 кЕ) при кімнатній температурі.

Ключові слова : упорядкування катіонів, манганіти, магнітоопір.

МАГНИТОСОПРОТИВЛЕНИЕ ПРИ КОМНАТНОЙ ТЕМПЕРАТУРЕ В МАНГАНИТАХ $Pr_{0.70}Ba_{0.30}MnO_{3+\delta}$ С УПОРЯДОЧЕНИЕМ В А-ПОЗИЦИИ

С. В. Труханов, А. В. Труханов, С. Е. Botez, H. Szymczak

Аннотация. Исследованы структура и магнитотранспортные свойства упорядоченного состояния в А-позиции в манганитах $Pr_{0.70}Ba_{0.30}MnO_{3+\delta}$ ($\delta = 0, 0.025$). Исходный разупорядоченный в А-позиции состав $Pr_{0.70}Ba_{0.30}MnO_3$ является орторомбическим (SG = Imma, Z = 4) ферромагнетиком с температурой Кюри $T_C \approx 173$ K. Он проявляет два пика электрического сопротивления при $T_I \sim 128$ K и $T_{II} \sim 173$ K, а также два пика магнитосопротивления ~ 74 % и ~ 79 % в поле 50 кЭ. Этот образец $Pr_{0.70}Ba_{0.30}MnO_3$ состоит из кристаллитов со средним размером $\langle D \rangle \approx 10.213$ μm. Последовательный отжиг этого образца в вакууме $P[O_2] \approx 10^{-4}$ Па и затем на воздухе при $T = 800\ ^0C$ ведет к разрушению его начальной структуры и химическому расслоению на две фазы: (i) стехиометрической по кислороду упорядоченной в А-позиции $PrBaMn_2O_6$ с тетрагональной (SG = P4/mmm, Z = 2) элементарной ячейкой и $T_C \approx 313$ K и (ii) сверхстехиометрической по кислороду разупорядоченной в А-позиции $Pr_{0.90}Ba_{0.10}MnO_{3.05}$ с орторомбической (SG = Pnma, Z = 4) элементарной ячейкой и $T_C \approx 133$ K. Он также проявляет магнитосопротивление ~ 14 % при ~ 313 K в поле 50 кЭ. Этот образец состоит из кристаллитов с уменьшенным средним размером $\langle D \rangle \approx 491$ nm. Наблюдаемые магнитные свойства интерпретируются в предположении химического фазового расслоения, а также эффектов размерности кристаллитов и упорядочения катионов в А-позиции. Полученные в данной работе материалы могут быть использованы при создании датчиков магнитного поля, так как обладают значительным магнитосопротивлением (~14% в поле 50 кЭ) при комнатной температуре.

Ключевые слова : упорядочение катионов, манганиты, магнитосопротивление.

Complex manganese oxides $Ln_{1-x}D_xMnO_3$, where Ln − trivalent lanthanide, D − divalent alkaline earth metal, with perovskite structure have been extensively investigated [1] due to their remarkable electrical and magnetic properties that include the so-called colossal magnetoresistive effect [2]. While many factors determine the properties of manganites, the most important ones are their electronic structure, which is related to the ion type and stoichiometry, and their crystal structure, where the average $\langle Mn - O \rangle$ bond length and the average $\langle Mn - O - Mn \rangle$ bond angle play key roles. For these materials the decrease of the lanthanide ion radius leads to decrease of the average $\langle Mn - O - Mn \rangle$ bond angle from 180° [3], and to the reduction of both the e_g-electron bandwidth, $W = \cos(1/2[\pi - \langle Mn - O - Mn \rangle]) / \langle Mn - O \rangle^{3.5}$ and the e_g-electron transfer integral $b_{ij} = b_{ij}^0 \cos(\theta_{ij}/2)$ [4]. Here, $b_{ij}^0 \sim \langle Mn - O - Mn \rangle$ and θ_{ij} is the angle between neighboring S_i and S_j spins. For complex doped $Ln_{1-x}D_xMnO_3$ manganites increasing the dopant concentration x induces a transformation from an antiferromagnetic insulator to a ferromagnetic metal. The maximum values of T_C are reached for the optimal doping x ~ 0.3 [1]. Moreover, for a given hole concentration the magnetotransport properties of the doped manganites are determined not only by the average A-site ionic radius $\langle r_A \rangle = (1-x)r_{Ln} + xr_D$, but also by the size mismatch at the A site represented by the variance $\sigma^2 = \sum x_i r_i^2 - \langle r_A \rangle^2$ (where i is A-site cation type) [5]. Several theoretical models have been developed in an attempt at explaining the physical properties of complex manganites, including double exchange interactions, superexchange interactions, or phase separations with competitive exchange interactions having opposite signs [6]. Cation ordering in the perovskite structure is known to noticeably alter the magnetotransport properties of manganites even when $\langle r_A \rangle$ and σ^2 have fixed values. The A-site disordered solid solution series $Pr_{1-x}Ba_xMnO_3$ and $Nd_{1-x}Ba_xMnO_3$ exhibit the maximum values of T_C (176 K [7] and 151 K [8]) for x ~ 0.30. Disordered $Pr_{0.50}Ba_{0.50}MnO_3$ and $Nd_{0.50}Ba_{0.50}MnO_3$ (x=0.50) have lower T_C values: ~ 140 K [9] and ~ 80 K [10], respectively. However, the A-site ordered compounds $PrBaMn_2O_6$ and $NdBaMn_2O_6$ (where the A-type antiferromagnetic state is the basic magnetic one) show ferromagnet-paramagnet transitions at ~ 320 K and ~ 310 K [10]. It is interesting to note that such properties are observed only for manganites with the maximal (100%) degree of Ln^{3+} and

Ba^{2+} cations ordering. Using special conditions of treatment a series of solid solutions $[Ln_gBa_{1-g}]_{Ln}[Ln_{1-g}Ba_g]_{Ba}Mn_2O_6$ with various degrees of the A-site ordering from 0 to 100% has been obtained [11]. In this case the partial A-site disordering suppresses the antiferromagnetism and, as a result, the La^{3+}-, Pr^{3+}-, and Nd^{3+}-based solid solutions become pure ferromagnets. Yet, the minimal value of the Ba^{2+} cation concentration for which the A-site ordered state can be formed, as well as the synthesis and microscopic details of such a state have been not determined so far. Here we present the results of our investigation on the structure and magnetotransport properties of A-site disordered and ordered phases in optimally doped $Pr_{0.70}Ba_{0.30}MnO_{3+\delta}$ ($\delta = 0$ and 0.025) manganites with fixed $\langle r_A \rangle = 1.2663$ Å, $\sigma^2 = 0.0178$ Å^2.

The polycrystalline oxygen stoichiometric A-site disordered $Pr_{0.70}Ba_{0.30}MnO_3$ sample has been obtained using conventional ceramic technology. Oxides Pr_6O_{11} and Mn_2O_3 as well as carbonate $BaCO_3$ (all of high-purity grade) have been weighed in accordance with the cation ratio and thoroughly mixed. Decarbonization and compaction of the ceramic have been carried out by annealing the sample in air for 2 h at T = 1100 °C, followed by crushing. The final synthesis has been carried out in air at T = 1560 °C for 2 h. Then it was slowly cooled down to room temperature at a rate of 100 °C/1 h to obtain an oxygen content close to the stoichiometric value. The anion-deficient sample has been obtained by the topotactic reaction. The sample has been placed in an evacuated (P ~ 10^{-4} Pa) and fused quartz ampoule together with a certain amount of metallic tantalum, which has been used as an oxygen getter. The quartz ampoule containing the sample has been kept for 24 h at T = 800 °C and then cooled to room temperature at a rate of 100 °C/1 h. Reduction has been carried out to the phase " $O_{2.60}$ " to satisfy the condition $Mn^{3+}/Mn^{2+} = 1$. The oxygen content of the anion-deficient $Pr_{0.70}^{3+} Ba_{0.30}^{2+} Mn_{0.50}^{3+} Mn_{0.50}^{2+} O_{2.60}^{2-}$ sample has been determined by weighing before and after the reaction. The anion-deficient sample was then subjected to oxidation in air for 5 h at T = 800 °C to obtain the nominal phase " O_3 ". After oxidation the oxygen content has been monitored by weighing as well as by chemical titration and it has been determined to be 3.025 ± 0.001. The chemical composition of all the samples has been studied by a PHI Model 660 scanning Auger microprobe. X-ray diffraction phase analysis has been carried out on a DRON-

3M diffractometer using the Cu-K$_\alpha$ radiation in the angular interval $20 \deg \leq 2\Theta \leq 80 \deg$. The X-ray diffraction patterns have been analyzed by the Rietveld method using the FullProof software. Grain topography imaging was carried out using a Carl Zeiss LEO1455VP scanning electron microscope. The dc-resistivity of the samples has been measured by standard four probe technique over a temperature range 3-350 K. Indium eutectic has been employed to deposit the contacts. The magnetoresistance has been calculated according to the relation: $MR = \{[\rho(H) - \rho(H=0)] / \rho(H=0)\}*100\%$, where MR is the negative isotropic magnetoresistance, $\rho(H)$ the resistivity in a magnetic field of 50 kOe, and $\rho(H=0)$ the resistivity without a magnetic field.

The analysis of the X-ray diffraction patterns shown in Fig.1-a indicates that the oxygen stoichiometric A-site disordered $Pr_{0.70}Ba_{0.30}MnO_3$ sample is well described ($\chi^2 = 2.77$) by an orthorhombic (SG = Imma, Z = 4) perovskite-like unit cell (Fig. 2-a) with parameters a = 5.5252(7) Å, b = 7.7672(8) Å, c = 5.5076(7) Å and V = 236.36(6) Å^3. These results are in good agreement with previous data [12]. The X-ray diffraction patterns for the oxygen superstoichiometric A-site ordered $Pr_{0.70}Ba_{0.30}MnO_{3.025}$ sample (Fig. 1-b) can be satisfactorily calculated ($\chi^2 = 2.91$ (2.91)) only if two phases are considered: (i) oxygen stoichiometric A-site ordered $PrBaMn_2O_6$ with a tetragonal (SG = P4/mmm, Z = 2) unit cell and (ii) oxygen superstoichiometric A-site disordered $Pr_{0.90}Ba_{0.10}MnO_{3.05}$ with an orthorhombic (SG = Pnma, Z = 4) unit cell. This is also in good agreement with previous data. The volume ratio of the two phases is $V(PrBaMn_2O_6)/V(Pr_{0.90}Ba_{0.10}MnO_{3.05}) \sim 1$. The use of the Imma or Pnma one-phase mode and/or P4/mmm+Imma two-phase mode as well as the disregard of the tetragonal space group P4/mmm considerably lower the quality of the Rietveld refinement. The presence of the tetragonal group P4/mmm indicates that the cation ordering is preserved. This type of distortion (SG = P4/mmm, Z = 2) is associated with ordering of Pr^{3+} and Ba^{2+} cations in the (001) planes which implies the unit cell doubling along the [001] direction. Direct proof of cation ordering is the presence of (0 0 1/2) reflections in the X-ray diffraction patterns, as well as the results of earlier electron diffraction and high resolution electron microscopy experiments on $PrBaMn_2O_{5.70}$ [10]. Worthy of note is that the ordering of Pr^{3+} and Ba^{2+} cations not only reduces the comparable unit cell volume of A-site ordered

phase by approximately 1% but also increases the average $\langle Mn - O - Mn \rangle$ bond angle by approximately 6 %. It will be shown below that such minimal changes in the crystal structure considerably modify the magnetoresistance properties.
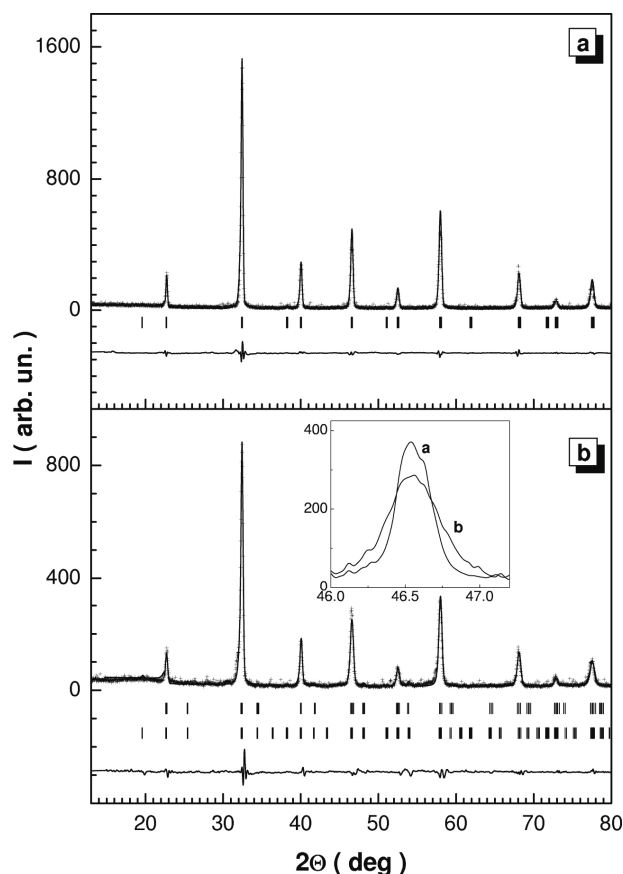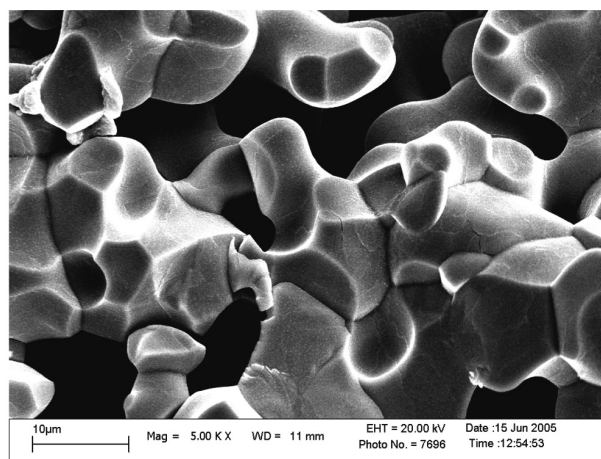

Fig. 1. The diagram of powder X-ray diffraction at room temperature for the oxygen stoichiometric A-site disordered $Pr_{0.70}Ba_{0.30}MnO_3$ **(a)** and oxygen superstoichiometric A-site ordered $Pr_{0.70}Ba_{0.30}MnO_{3.025}$ **(b)** samples. Experimental data (dark circles), fitting curve (solid curve), admissible positions of Bragg reflections (vertical segment) and the difference curve (lower solid curve). Insert demonstrates the shape and widening of the Bragg reflections.
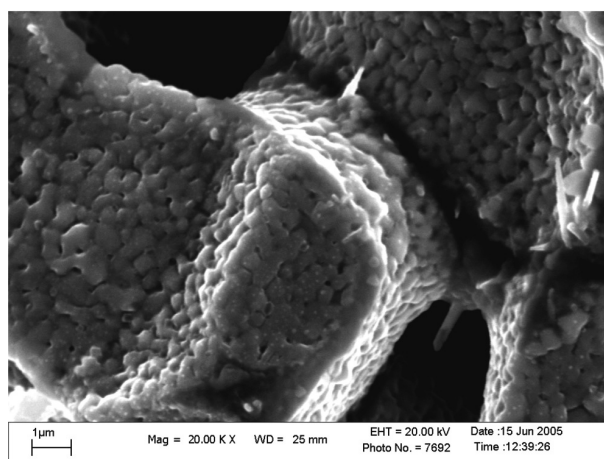
Fig. 2 shows the grain topography obtained by scanning electron microscopy for the oxygen stoichiometric A-site disordered $Pr_{0.70}Ba_{0.30}MnO_3$ and oxygen superstoichiometric A-site ordered $Pr_{0.70}Ba_{0.30}MnO_{3.025}$ samples. The noticeable decrease in the average grain size for the oxygen superstoichiometric A-site ordered $Pr_{0.70}Ba_{0.30}MnO_{3.025}$ sample (after the reduction-reoxidization reaction) from micrometer to nanometer size can be explained by the intense diffusion of ions as well as by the ordering of the oxygen vacancies in the shape of complex surfaces over which the destruc-

tion of the material occurs. As it can be observed, the nanograins combine to form a mosaic structure spanning the entire ceramic. The grain size variation interval for the oxygen superstoichiometric A-site ordered $Pr_{0.70}Ba_{0.30}MnO_{3.025}$ sample is $0.254 \div 0.901$ μm, whereas its counterpart for the oxygen stoichiometric A-site disordered $Pr_{0.70}Ba_{0.30}MnO_3$ is $3.817 \div 17.540$ μm. The quantitative stereologic analysis of the oxygen stoichiometric A-site disordered $Pr_{0.70}Ba_{0.30}MnO_3$ sample shows that 19.36 % of the grains have a size variation from 10.000 μm to 12.000 μm. The average grain size is $\langle D \rangle \approx 10.213$ μм. Grains with sizes smaller 0.200 μm or larger 18.000 μm have been not detected. For the oxygen superstoichiometric A-site ordered $Pr_{0.70}Ba_{0.30}MnO_{3.025}$ 44.30 % of the grains have a size variation from 0.400 μm to 0.600 μm. Grains with size smaller 0.100 μm and larger 1.000 μm have been not detected. The average grain size for this sample is $\langle D \rangle \approx 0.491$ μм. The shape of the Bragg peaks is affected by the small grain size, which is observed on insert of Fig.1. The A-site ordered $Pr_{0.70}Ba_{0.30}MnO_{3.025}$ sample with nanograines demonstrates the wide Bragg peaks. The size of the crystallites influences the properties of the crystal structure. A decrease in the grain size (to nanometer size) reduces the unit cell volume, which can be explained by an increase in the surface tension as compared to elastic forces in the bulk material [13]. This follows from comparison of the commensurate unit cell volume of the $Pr_{0.90}Ba_{0.10}MnO_{3.05}$ phase (in our case $V = 236.60(5)$ Å^3) to the previous results ($V = 238.44(7)$ Å^3). We concluded that the decrease in the unit cell volume in the oxygen superstoichiometric A-site ordered $Pr_{0.70}Ba_{0.30}MnO_{3.025}$ samples occurs as a result of both cation ordering and an increase of surface tension in the outside layers of the nanograines. The oxygen stoichiometric A-site disordered $Pr_{0.70}Ba_{0.30}MnO_3$ sample is a ferromagnet with Curie temperature $T_C \sim 173$ K. At the same time, the oxygen superstoichiometric A-site ordered $Pr_{0.70}Ba_{0.30}MnO_{3.025}$ sample exhibits two magnetic transitions at ~ 313 K and ~ 133 K. These correspond to the transition from the paramagnetic to the ferromagnetic state for the oxygen stoichiometric A-site ordered $PrBaMn_2O_6$ and oxygen superstoichiometric A-site disordered $Pr_{0.90}Ba_{0.10}MnO_{3.05}$ phases, respectively. For this sample, the phase transitions are not particularly sharp, which suggests an incomplete ordering of the Pr^{3+} and Ba^{2+} cations in the $PrBaMn_2O_6$ phase. The oxygen superstoichiometric A-site disordered $Pr_{0.90}Ba_{0.10}MnO_{3.05}$ exhibits

slightly higher values of $T_C \sim 133$ K as compared to the available literature value of $T_C \sim 110$ K, which can be attributed to the above-discussed nanocrystallite compression and to the presence of the superstoichiometric Mn^{4+} cations.

Fig. 2. The grain topography obtained with the help of a scanning electron microscope for the oxygen stoichiometric A-site disordered $Pr_{0.70}Ba_{0.30}MnO_3$ **(a)** and oxygen superstoichiometric A-site ordered $Pr_{0.70}Ba_{0.30}MnO_{3.025}$ **(b)** samples.

Fig. 3 illustrates the temperature dependence of the electrical resistivity and magnetoresistance measured in magnetic field of 50 kOe. The oxygen stoichiometric A-site disordered $Pr_{0.70}Ba_{0.30}MnO_3$ exhibits a semiconductor behavior in the paramagnetic state above ~ 173 K (Fig. 3-a). This sample has two peaks of electrical resistivity, at $T_I \sim 128$ K and $T_{II} \sim 173$ K. The temperature ~ 173 K coincides with the Curie temperature T_C. Below T_C the ferromagnetic order decreases via magnetoimpurity scattering of the charge carriers and the conductiv-

ity shows a metallic behavior. The resistivity peak at $T_I \sim 128$ K for the oxygen stoichiometric A-site disordered $Pr_{0.70}Ba_{0.30}MnO_3$ sample can not be explained by spin-dependent tunneling of the charge carriers between grains because the grains are in the micrometer range and the grain boundaries bring in a small contribution to the resistivity [14]. However, above-mentioned peak at $T_I \sim 128$ K may be explained by magnetic phase separation in the ferromagnetic and paramagnetic clusters. In Ref. [15] the equation for the total resistivity in the ferromagnetic state has been obtained as :

$$\frac{\varphi_P(R^{-g} - R_P^{-g})}{R^{-g} + KR_P^{-g}} + \frac{(1-\varphi_P)(R^{-g} - R_F^{-g})}{(R^{-g} + KR_F^{-g})} = 0$$
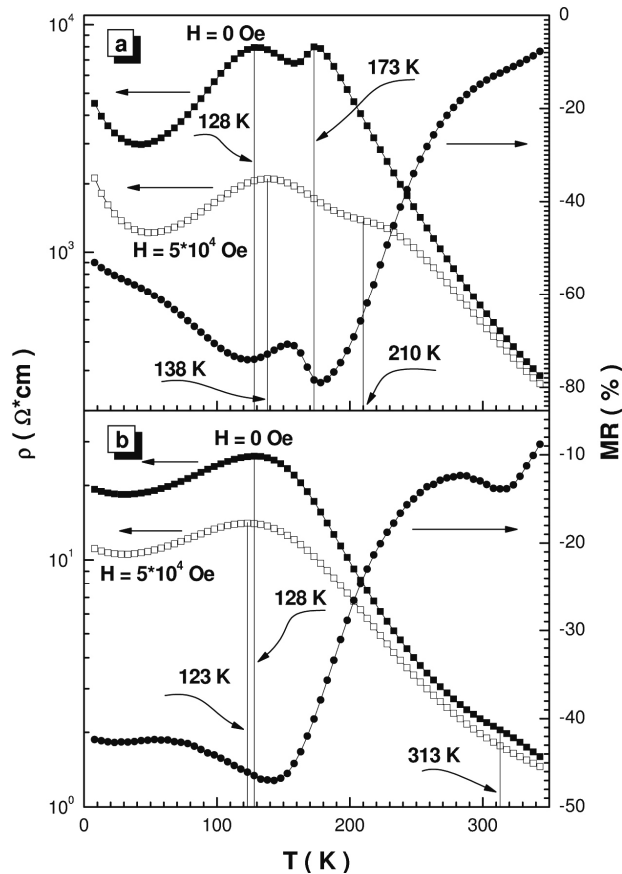

Fig. 3. The temperature dependence of the electrical resistivity in absence magnetic field (full rectangles) and in field of 50 kOe (open rectangles) as well as magnetoresistance (full circles) for the oxygen stoichiometric A-site disordered $Pr_{0.70}Ba_{0.30}MnO_3$ **(a)** and oxygen superstoichiometric A-site ordered $Pr_{0.70}Ba_{0.30}MnO_{3.025}$ **(b)** samples.

Here R is the total resistivity, $R_F = B + C(T/T_C)^2$ is the resistivity in ferromagnetic state (where $(dR_F/dT > 0)$, and B and C are constants), and $R_P = A(T/T_C)exp(E_{AC}T_C/T)$ is resistivity in the paramagnetic state (where $(dR_P/dT < 0)$ and A is constant). E_{AC} is the polaron activation energy, and ϕ_P the volume fraction of the paramegnetic phase (where $\phi_P = 1$ at $T > T_C$ and $\phi_P = exp[(T/T_C - 1)/d]$, with d the critical parameter of ferromagnet-paramagnet phase transition and K and g constants which determine the percolation threshold). An electrical resistivity anomaly should be observed at the widening of the ferromagnet-paramagnet transition, below T_C. Also, for $d \geq 3.2$ on the resistivity curve, below T_C, the second peak appears. That is observed in our experiments. Switching on the magnetic field reduces the resistivity and increases the resistivity peak temperatures to $T_I \sim 138$ K and $T_{II} \sim 210$ K (Fig. 3-a). The presence of the magnetic field also induces two peaks in the magnetoresitance: ~ 74 % and ~ 79 %. In addition, the A-site ionic ordering leads to the increase of the metal-insulator transition temperature. For the oxygen superstoichiometric A-site ordered $Pr_{0.70}Ba_{0.30}MnO_{3.025}$ sample (Fig. 3-b) the transition temperatures are $T_I \sim 128$ K and $T_{II} \sim 313$ K. The high-temperature peak almost disappears in a magnetic field, and the magnetoresistance at ~ 313 K is 14 %. The increase of the resistivity transition temperature for the oxygen superstoichiometric A-site ordered $Pr_{0.70}Ba_{0.30}MnO_{3.025}$ sample is probably due to the increase the e_g-electron bandwidth $W = cos(1/2[\pi - \langle Mn - O - Mn \rangle]) / \langle Mn - O \rangle^{3.5}$ and e_g-electron transfer integral $b_{ij} = b_{ij}^0 cos(\theta_{ij}/2)$. The materials obtained in this work may be used at the creation of the magnetic field sensors, as they have considerable magnetoresistance ($\sim 14\%$ in field of 50 kOe) at room temperature. This study has been partly supported by the Belarus Republic Foundation for Basic Research (grants no. F08R-148 and F09K-015).

References

1. Jonker G.H., Van Santen J.H. Ferromagnetic compounds of manganese with perovskite structure. // Physica (Utrecht). — 1950. — 16. — 337-349.
2. Giant negative magnetoresistance in perovskite-like $La_{2/3}Ba_{1/3}MnO_x$ ferromagnetic films. / R. Von Helmolt, J. Wecker, B. Holzepfel et al. // Phys. Rev. Lett. — 1993. — 71. — 2331-2333.
3. Sundaresan A., Maignan A., Raveau B. Effect of A-site cation size mismatch on charge ordering and colossal magnetoresistance properties of perovskite manganites. // Phys. Rev. B. — 1997. — 56. — 5092-5095.
4. High pressure neutron diffraction study of the metallization process PrNiO$_3$. / M. Medarde, J. Mesot,

P. Lacorre et al. // Phys. Rev. B. — 1995. — 52. — 9248-9258.

5. Rodriguez-Martinez L.M., Attfield J.P. Cation disorder and the metal-insulator transition temperature in manganese oxide perovskites. // Phys. Rev. B. — 1998. — 58. — 2426-2429.

6. Dagotto E., Hotta T., Moreo A. Colossal magnetoresistant materials: the key role of phase separation. // Phys. Repts. — 2001. — 344. — 1-153.

7. Comparative study of the magnetic and electrical properties of $Pr_{1-x}Ba_xMnO_{3-\delta}$ manganites depending on the preparation conditions. / S.V. Trukhanov, I.O. Troyanchuk, I.M. Fita et al. // J. Magn. Magn. Mater. — 2001. — 237. — 276-282.

8. Investigation of magnetic phase transformations in a system of $Nd_{1-x}Ba_xMnO_{3-\delta}$ ($0 \leq x \leq 0.50$) depending on the conditions of preparation. / S.V. Trukhanov, I.O. Troyanchuk, D.D. Khalyavin et al. // JETP. — 2002. — 94. — 329-335.

9. Effect of oxygen content on the magnetic and transport properties of $Pr_{0.5}Ba_{0.5}MnO_{3-\gamma}$. / I.O. Troyanchuk, S.V. Trukhanov, H. Szymczak, K. Bärner. // J. Phys.: Condens. Matter. — 2000. — 12. — L155-L158.

10. Magnetic and electrical properties of $LBaMn_2O_{6-\gamma}$ (L = Pr, Nd, Sm, Eu, Gd, Tb) manganites. / S.V. Trukhanov, I.O. Troyanchuk, M. Hervieu et al. // Phys. Rev. B. — 2002. — 66, 184424-4.

11. Trukhanov S.V. Investigation of stability of ordered manganites. // JETP. — 2005. — 101. — 513-520.

12. Vacancy effects on the physical properties in lacunar $Pr_{0.7-x}Ba_{0.3}MnO_3$ oxides. / W. Boujelben, A. Cheikh-Rouhou, M. Ellouze, J.C. Joubert. // J. Magn. Magn. Mater. — 2002. — 242. — 662-664.

13. Enhanced ferromagnetic transition temperature in nanocrystalline lanthanum calcium manganese oxide ($La_{0.67}Ca_{0.33}MnO_3$). / K.S. Shankar, S. Kar, G.N. Subbanna et al. // Solid State Commun. — 2004. — 129. — 479-483.

14. Ju H.L., Sohn H. Role of grain boundaries in double exchange manganite oxides $La_{1-x}A_xMnO_3$ (A = Ca, Ba). // Solid State Commun. — 1997. — 102. — 463-466.

15. Tovstolytkin A.I., Pogorilyi A.N., Kovtun S.M. Double-peaked character of the temperature dependence of resistance of perovskite manganites for a broadened ferromagnetic transition. // Low Temperature Physics. — 1999. — 25. — 962-965.